

Short Communication

Evaluating autologous peritoneum grafting for enhanced healing of bile duct injuries: A preliminary data from an animal study

Anung N. Nugroho^{1*}, Ambar Mudigdo^{1,2,3}, Soetrisno Soetrisno^{1,4,5}, Kristanto Y. Yarso⁶, Ida Nurwati^{1,7}, Dono Indarto⁸ and Eti P. Pamungkasari^{1,9}

¹Doctoral Program of Medical Sciences, Faculty of Medicine, Universitas Sebelas Maret, Surakarta, Indonesia; ²Department of Anatomical Pathology, Faculty of Medicine, Universitas Sebelas Maret, Surakarta, Indonesia; ³Department of Anatomical Pathology, Dr. Moewardi Hospital, Surakarta, Indonesia; ⁴Department of Obstetrics and Gynecology, Faculty of Medicine, Universitas Sebelas Maret, Surakarta, Indonesia; ⁵Department of Obstetrics and Gynecology, Dr. Moewardi Hospital, Surakarta, Indonesia; ⁶Division of Oncology, Department of Surgery, Universitas Sebelas Maret, Surakarta, Indonesia; ⁷Department of Acupuncture, Faculty of Medicine, Universitas Sebelas Maret, Surakarta, Indonesia; ⁸Department of Physiology and Biomedical Laboratory, Universitas Sebelas Maret, Surakarta, Indonesia; ⁹Department of Public Health, Faculty of Medicine, Universitas Sebelas Maret, Surakarta, Indonesia

*Corresponding author: notonugroho@student.uns.ac.id

Abstract

Increased incidence of laparoscopic cholecystectomy-related bile duct injuries (BDIs), combined with its risk of serious complications and mortality, highlights the need for a more effective repair technique. Although the use of autologous graft in BDI repair has been promoted, the role of autologous parietal peritoneum remains underexplored. The aim of this study was to evaluate the effect of autologous parietal peritoneum grafts in rabbit models of partial BDI, emphasizing its effect on the expression of cluster of differentiation 68 (CD68) and transforming growth factor- β (TGF- β). An experimental post-test-only design was employed, using 27 male New Zealand rabbits (*Oryctolagus cuniculus*) aged 8–10 months. The rabbits were allocated into three groups: control (primary closure), autologous parietal peritoneum graft, and autologous gallbladder graft. Partial BDI measuring 15×5 mm were surgically created and repaired according to group assignments. The expression of CD68 and TGF- β were measured via enzyme-linked immunosorbent assay (ELISA), while the anastomosis was pathologically examined through hematoxylin and eosin (H&E) staining on days 3, 7, and 14 post-surgery. Statistical analysis was performed using analysis of variance (ANOVA) followed by Bonferroni post hoc tests. No statistically significant difference was observed in the expression of CD68 or TGF- β among the three treatment groups on days 3, 7, and 14 post-surgery, indicating that the effects of autologous parietal peritoneum graft were comparable to the control and the autologous gallbladder graft in promoting wound healing. Fibroblast density on day 3 was significantly lower in the parietal peritoneum group ($p=0.040$), reflecting delayed recruitment, but normalized by day 14, indicating successful integration and remodeling. The study highlights the potential role of autologous parietal peritoneum grafts for BDI.

Keywords: Bile duct injury, autologous parietal peritoneum, TGF- β , CD68, fibroblasts

Introduction

Bile duct injury (BDI) is a serious complication predominantly associated with hepatobiliary surgeries, with laparoscopic cholecystectomy as the leading contributor [1]. The transition from open to laparoscopic cholecystectomy, while reducing overall surgical morbidity, has



paradoxically increased the incidence of BDI, with rates of 0.4–0.6% in laparoscopic surgeries compared to 0.1–0.2% in open procedures [2]. Although relatively infrequent, BDI significantly impacts patient outcomes, often leading to bile leakage, biliary strictures, cholangitis, and, in severe cases, liver failure, which collectively jeopardizes survival and quality of life [3].

Management strategies for BDI range from non-surgical methods, such as endoscopic stenting and percutaneous drainage for minor injuries, to surgical interventions for major injuries [4]. Surgical options like primary end-to-end anastomosis and biliary-enteric reconstruction (e.g., Roux-en-Y hepaticojejunostomy) are considered standard treatments. However, complications often hinder these approaches, including anastomotic failure, strictures, and ischemic tissue damage, especially in complex cases [5].

In response to these challenges, autologous grafts have emerged as a novel alternative for enhancing BDI repair. Harvested from the patient's tissues, autologous grafts minimize the risk of immunogenic rejection and are more likely to integrate with native tissues [6]. Various types, including vein [7], intestinal [8], and ureteral grafts [9] have been explored. Vein grafts offer flexibility and patency but are limited by availability and thrombosis risk [7]. Intestinal grafts have been explored in biliary reconstruction and may pose challenges, including risks of infection and cholangitis [8]. These limitations highlight the need for an optimal graft material that combines biocompatibility, accessibility, and regenerative potential [10].

The autologous peritoneum represents a promising but underutilized grafting material for BDI repair. This serous membrane, readily accessible during abdominal surgeries, offers several advantages, including a rich vascular supply, pro-angiogenic properties, and regenerative capacity [11]. Preliminary evidence suggests that peritoneal grafts yield favorable outcomes in vascular [12] and urologic surgeries [13]. However, their application in BDI repair remains largely unexplored, with no systematic investigations evaluating their efficacy in promoting bile duct healing, reducing inflammation, or enhancing tissue regeneration [14]. To date, no experimental or clinical studies have systematically assessed the impact of autologous peritoneum grafts on bile duct healing, particularly in terms of inflammatory markers, tissue regeneration, and angiogenesis. The aim of this study was to investigate the impact of autologous parietal peritoneum grafts on BDI in animal models, with a specific focus on the expression of cluster of differentiation 68 (CD68) and transforming growth factor- β (TGF- β) as markers of inflammation and fibrosis, respectively.

Methods

Study design and setting

A true experimental post-test-only control group design was conducted to assess the effects of the autologous parietal peritoneum and gallbladder grafts on bile duct repair, at the Laboratory of Surgery, Faculty of Veterinary Medicine, Universitas Gadjah Mada, Yogyakarta, Indonesia. Data collection and sample acquisition were carried out between December 2023 and January 2024, using the New Zealand rabbits (*Oryctolagus cuniculus*) as a preclinical model to evaluate healing outcomes, focusing on inflammatory and regenerative markers, including CD68, TGF- β , and fibroblasts.

Animal preparation

The study population consisted of adult male New Zealand rabbits aged 8–10 months, weighing between 2.0 and 3.0 kg. Rabbits were excluded from the study if they exhibited illness prior to or during the research period or had been used previously in any study. The animals were sourced from the accredited breeding facility at Prof. Soeparwi Veterinary Hospital, Faculty of Veterinary Medicine, Universitas Gadjah Mada, which maintains high ethical standards for animal care. Inclusion criteria were strictly applied to ensure uniformity in the study cohort.

Sample size and allocation

Sample size determination followed Federer's formula, requiring a minimum of three rabbits per group to achieve statistical reliability. A total of 41 rabbits met the inclusion criteria and were

assigned to one of the three groups: the control group, the parietal peritoneum graft group, and the gallbladder graft group.

Animal acclimatization and housing

Prior to inclusion, a thorough health screening was performed to ensure the absence of systemic or localized diseases. Following selection, the rabbits underwent a 7-day acclimatization period, during which they were housed in a controlled environment maintained at 27°C, with a 12-hour light/dark cycle to mimic natural conditions. A standard commercial rabbit diet was provided, alongside unrestricted access to water to maintain hydration. Deworming was performed using albendazole (20–50 mg/kg, orally), administered once at the start of the acclimatization period. A fasting period of 4 to 8 hours was observed prior to the surgical procedures to standardize conditions for the interventions. Any rabbits that exhibited signs of illness, died during the study or had prior experimental exposure were excluded from the study to minimize confounding factors.

Despite careful monitoring and handling, a total of 11 rabbits were excluded from the study due to mortality occurring prior to the collection of anastomosis tissue samples. Mortality was primarily attributed to bile duct leakage, as confirmed through post-mortem autopsies. The distribution of fatalities was as follows: three rabbits from the control group, three from the parietal peritoneum graft group, and five from the gallbladder graft group.

Experimental groups

The rabbits were randomly assigned into three experimental groups (Groups A, B, and C), with each group containing nine animals. Group A, the control group, underwent bile duct repair via primary closure without grafting. Group B, the parietal peritoneum graft group, involved excising a 1.5 cm segment of the bile duct, which was subsequently repaired using an autologous parietal peritoneum graft, with a 5 cm stent placed to ensure continuous bile flow. Group C, the gallbladder graft group, also involved the excision of a 1.5 cm bile duct segment, followed by repair using an autologous gallbladder graft, similarly supported by a 5 cm stent to maintain bile duct patency. Healing progression in all groups was assessed at three distinct postoperative time points: day 3 (inflammatory phase), day 7 (transition/proliferative phase), and day 14 (remodeling phase), to evaluate the dynamics of tissue healing and graft integration. All procedures were conducted in accordance with the guidelines established by the Johns Hopkins University Animal Care and Use Committee (JHU ACUC), ensuring ethical standards and animal welfare [15].

Animal model and intervention

The rabbits were anesthetized using intravenous injections of ketamine (50 mg/kg) and dexmedetomidine (1–2 mg/kg). Maintenance of anesthesia was achieved through inhalation of 2% halothane combined with 100% oxygen. The animals were positioned in the supine decubitus position, and anesthesia was sustained with a vaporizer administering isoflurane and sevoflurane. A midline laparotomy was performed to access the abdominal cavity, exposing the common bile duct. A segment of the parietal peritoneum was then excised from the abdominal wall, and measured precisely to dimensions of 15×5 mm to match the bile duct defect. A standardized defect of the same dimensions was created in the anterior wall of the bile duct using fine surgical scissors. Anastomosis was then performed by grafting the peritoneal segment over the defect, ensuring a stable and secure repair, as indicated by the white arrow in **Figure 1**.

In Group A (control), the defect was repaired using simple interrupted sutures with 7-0 polypropylene. In Group B, a parietal peritoneum segment was harvested, trimmed to match the defect, and grafted over it using interrupted sutures with 7-0 polypropylene. A 5F stent was inserted into the bile duct lumen to maintain patency during the healing process. In Group C, a gallbladder graft was prepared by excising a segment of the gallbladder, which was shaped and sutured to cover the bile duct defect using the same technique as in Group B. A 5F stent was similarly inserted to maintain bile flow. All procedures were conducted under sterile conditions to minimize infection risk. Operative times were recorded, and surgical site handling was standardized across all groups to ensure consistency.

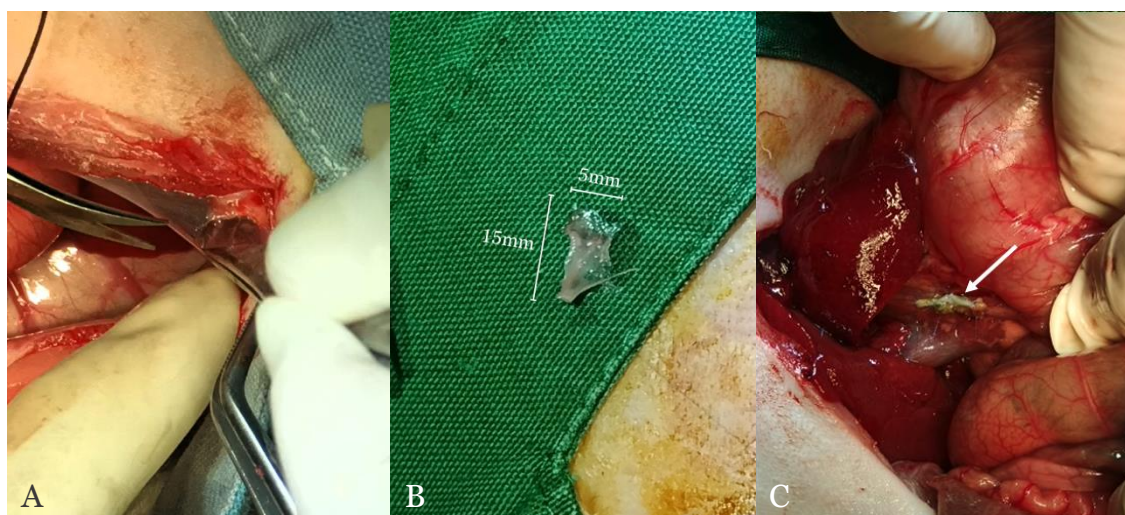


Figure 1. Steps in surgical procedure. (A) Excision of the parietal peritoneum from the abdominal wall. (B) Measurement of the peritoneum parietal at 15×5 mm. (C) Final appearance of the anastomosis (indicated by white arrow).

Postoperative care

The postoperative care protocols were standardized across all experimental groups to ensure consistency. Upon recovery, rabbits were administered intravenous isotonic saline to maintain adequate hydration levels. To prevent postoperative infections, a prophylactic regimen of ceftriaxone (25 mg/kg) was administered intramuscularly once daily for three consecutive days. The pain was managed using meloxicam (0.2 mg/kg), delivered subcutaneously once daily for three days. Rabbits were housed individually in clean, temperature-controlled cages to minimize stress and risk of cross-contamination. Monitoring was conducted twice daily to assess for signs of infection, including erythema and discharge, and for indications of bile leakage, such as abdominal distension. Additionally, food and water intake were closely monitored, and any deviations from normal consumption patterns were recorded and addressed.

Termination and sample collection

The rabbits were humanely euthanized on days 3, 7, and 14 using an overdose of pentobarbital sodium (100 mg/kg), administered intravenously. This euthanasia schedule was selected to coincide with key stages of tissue healing: inflammation (day 3), proliferation (day 7), and remodeling (day 14). Following euthanasia, a midline incision was performed to excise tissue samples from the bile duct, including a 20 mm segment of the adjacent tissue.

The collected tissues were immediately processed into two portions. One portion was fixed in 10% buffered formalin for histological analysis, which included hematoxylin and eosin (H&E) staining to assess fibroblast density and structural integrity. The second portion was homogenized and stored at -80°C for subsequent biochemical assays, including enzyme-linked immunosorbent assay (ELISA) to quantify biomarkers such as TGF- β , CD68, and fibroblast activity. Standardized tissue handling and storage protocols were implemented to maintain sample integrity and ensure reliable results for subsequent analyses.

Measurement of CD68

CD68 expression was quantitatively assessed using a rabbit-specific ELISA kit (BZ-08171420-EA; BioEnzy, Jakarta, Indonesia). Tissue samples from the bile duct and adjacent regions were excised and stored at -80°C until analysis to preserve protein integrity. For analysis, tissues were homogenized in a cold phosphate-buffered saline solution (pH: 7.4) to minimize protein degradation. The homogenization process was performed on ice to reduce enzymatic activity, and the resulting mixture was centrifuged at 3,000 rpm for 20 minutes at 4°C to remove cellular debris. The supernatant was carefully separated and stored at -20°C for subsequent ELISA analysis.

The CD68-specific ELISA was conducted using pre-coated plates optimized for the detection of the CD68 antigen. Plates were incubated at room temperature for two hours to allow the binding of CD68 in the sample to the antibody-coated wells. Following the incubation, the wells were washed three times with a wash buffer to remove any unbound substances. Biotinylated detection antibodies were then introduced to each well, and the plates were incubated for an additional hour at room temperature. After this second incubation, the plates underwent another series of washings to eliminate excess antibodies. The final detection step involved adding streptavidin conjugated to horseradish peroxidase (HRP) to each well, followed by a final incubation at room temperature for 30 minutes. The HRP enzyme catalyzed the conversion of the tetramethylbenzidine (TMB) substrate solution, producing a color change proportional to the amount of CD68 present in the samples. The reaction was terminated by adding a stop solution, and the optical density (OD) was measured at 450 nm using a microplate reader (Thermo Fisher Scientific, Waltham, USA). A standard curve, generated from known concentrations of recombinant CD68, was used to interpolate the concentrations of CD68 in the sample supernatants.

Measurement of TGF- β

TGF- β concentrations were measured using a highly sensitive rabbit-specific ELISA kit (BZ-22176822-EB, BioEnzy, Jakarta, Indonesia), following the manufacturer's instructions. Tissue samples were homogenized in a pre-chilled lysis buffer supplemented with a protease inhibitor cocktail to preserve cytokine integrity. The homogenates were subjected to centrifugation at 3,000 rpm for 20 minutes at 4°C. The resultant supernatant was carefully collected and stored at -20°C until further analysis. The OD of each well was measured at 450 nm using a microplate spectrophotometer (Thermo Fisher Scientific, Waltham, USA). Quantitative analysis was performed by interpolating sample OD values against a standard curve generated from serial dilutions of known TGF- β concentrations.

Measurement of fibroblast

Fibroblast activity was assessed via histological analysis using H&E staining to evaluate tissue remodeling and healing processes at bile duct repair sites. Tissue specimens were collected and fixed in 10% buffered formalin for 24–48 hours to preserve cellular and extracellular structures. The fixed samples were subjected to a sequential dehydration process using graded alcohol concentrations (70%, 80%, 95%, and 100%), cleared in xylene to remove lipids and impurities, and embedded in paraffin wax to create stable tissue blocks for sectioning.

Thin sections of 5 μ m thickness were obtained from the paraffin-embedded blocks using a microtome. The sections were carefully mounted on pre-cleaned glass slides, deparaffinized with xylene, and rehydrated through a descending alcohol series (100%, 95%, 80%, and 70%), followed by rinsing in distilled water to restore hydrophilic tissue properties. Hematoxylin staining was applied to selectively highlight nuclei in blue, while eosin staining rendered the cytoplasm and extracellular matrix in shades of pink.

Microscopic analysis was performed under a light microscope at 400 \times magnification. For quantitative assessment, fibroblast counts were conducted in five randomly selected high-power fields (HPFs) per sample. The mean fibroblast count per HPF was calculated to determine fibroblast density, which serves as a proxy for the extent of tissue remodeling and healing at the repair site. To ensure methodological rigor, all histological slides were independently reviewed by two experienced pathologists. Any discrepancies in fibroblast identification or counting were resolved through consensus discussions after joint slide examination. In addition, histopathological analysis was also conducted qualitatively.

Statistical analysis

Statistical analyses were performed using SPSS (IBM Corp., New York, USA) version 27. Data distribution normality was examined with the Shapiro-Wilk test, and Levene's test assessed the homogeneity of variances. For data that met normality and homogeneity criteria, one-way analysis of variance (ANOVA) was performed, followed by post-hoc least significant difference (LSD) analysis for pairwise comparisons. Non-normally distributed data were analyzed using the Kruskal-Wallis test, with Dunn's post-hoc test applied for subsequent pairwise assessments.

When normality was achieved, but homogeneity was violated, the Brown-Forsythe ANOVA was utilized, complemented by Dunnett T3 post-hoc analysis to address heteroscedasticity.

Parametric data were reported as mean \pm standard deviation (SD), while non-parametric data were expressed as medians with interquartile ranges (IQR). Statistical significance was determined using two-tailed tests, with a p -value threshold of <0.05 . Where appropriate, effect sizes were calculated to quantify the magnitude of significant differences, enhancing the interpretability of the results.

Results

Effects of autologous parietal peritoneum graft on TGF- β levels

TGF- β levels across the experimental groups on day 3, day 7, and day 14 are presented in **Table 1** and **Figure 2**. No significant differences were observed between groups, with p -values of 0.805, 0.576, and 0.982, respectively. Within-group analysis over time revealed no significant changes in TGF- β levels for the control group ($p=0.970$), parietal peritoneum graft group ($p=0.919$), or gallbladder graft group ($p=0.840$) across the three different time points. These findings indicated that TGF- β levels remained stable within all groups throughout the study.

Table 1. Comparison of TGF- β levels across experimental groups at different time points

Time points	TGF- β levels (pg/mL), mean \pm SD			p -value
	Control group (n=9)	Parietal peritoneum graft group (n=9)	Gallbladder graft group (n=9)	
Day 3	325.81 \pm 106.08	344.90 \pm 145.01	242.76 \pm 292.73	0.805 ^a
Day 7	295.72 \pm 187.68	270.73 \pm 3.45	144.86 \pm 201.57	0.576 ^a
Day 14	275.26 \pm 378.89	278.51 \pm 223.94	240.07 \pm 173.49	0.982 ^a
p -value	0.970 ^a	0.919	0.840 ^a	

SD: standard deviation; TGF- β : transforming growth factor- β

^aAnalyzed using ANOVA test

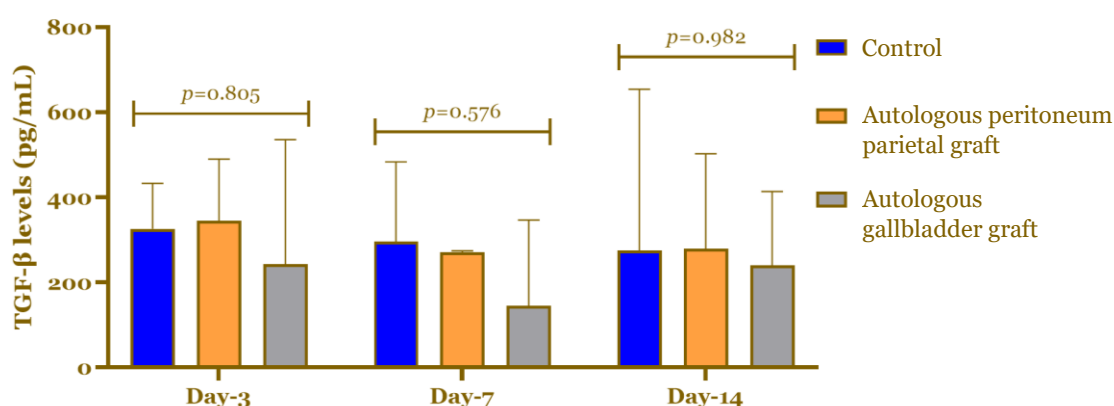


Figure 2. Comparison of mean levels of transforming growth factor- β (TGF- β) across experimental groups at different time points.

Effects of autologous parietal peritoneum graft on the CD68 levels

The levels of CD68 across the experimental groups are presented in **Table 2** and **Figure 3**. No statistically significant differences in CD68 expression were found between groups ($p=0.733$ on day 3, $p=0.403$ on day 7, and $p=0.933$ on day 14). Within-group analysis over time revealed no significant changes in CD68 levels for the control group ($p=0.395$), parietal peritoneum graft group ($p=0.587$), or gallbladder graft group ($p=0.594$) across days 3, 7, and 14. These findings indicate that CD68 expression remained stable within each group throughout the study period.

Fibroblast density quantification

Fibroblast density across experimental groups at different time points is presented in **Table 3** and **Figure 4**. A significant difference was observed on day 3 ($p=0.040$), with control group

showing a mean count of 21.00 ± 5.51 fibroblasts/HPF, significantly higher than parietal peritoneum graft group (8.67 ± 4.98 fibroblasts/HPF) but lower than gallbladder graft group (23.67 ± 6.67 fibroblasts/HPF). No significant differences were observed on days 7 and 14. Post-hoc analysis for day 3 revealed that fibroblast density in control group was significantly higher compared to parietal peritoneum graft group ($p=0.039$) and significantly lower compared to gallbladder graft group ($p=0.019$), while no significant difference was observed between the last two groups ($p=0.591$) (**Figure 2**).

Table 2. Comparison of CD68 levels across experimental groups at different time points

Time points	CD68 levels (pg/mL), mean \pm SD			p-value
	Control group (n=9)	Parietal peritoneum graft group (n=9)	Gallbladder graft group (n=9)	
Day 3	1.40 \pm 0.28	1.96 \pm 1.20	1.56 \pm 0.33	0.733 ^b
Day 7	0.61 \pm 0.67	1.93 \pm 1.50	1.16 \pm 1.00	0.403 ^a
Day 14	1.19 \pm 0.94	0.99 \pm 0.72	1.04 \pm 0.30	0.933 ^a
p-value	0.395 ^a	0.587 ^b	0.594 ^a	

CD68: cluster of differentiation 68; SD: standard deviation

^aAnalyzed using ANOVA test

^bAnalyzed using Kruskal-Wallis test

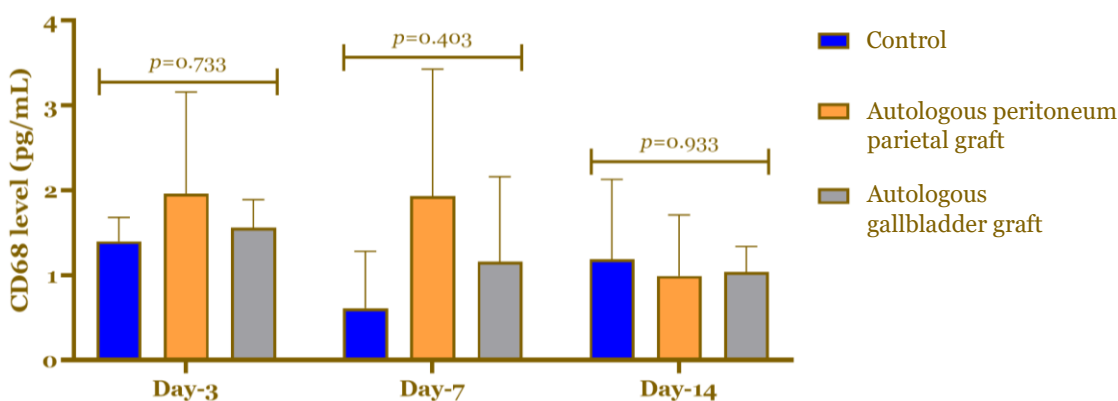


Figure 3. Comparison of mean levels of cluster of differentiation 68 (CD68) across experimental groups at different time points.

Within-group analysis over time revealed no significant differences in fibroblast number of control group ($p=0.430$), parietal peritoneum group ($p=0.060$), or gallbladder graft group ($p=0.731$) across three time points (**Table 3**). These findings suggest that while fibroblast number varied between groups at specific time points, it remained relatively stable within each group throughout the study period.

Table 3. Fibroblast density across experimental groups at different time points

Time points	Fibroblast number (fibroblasts/HPF at 400 \times), mean \pm SD			p-value
	Control group (n=9)	Parietal peritoneum graft group (n=9)	Gallbladder graft group (n=9)	
Day 3	21.00 \pm 5.51	8.67 \pm 4.98	23.67 \pm 6.67	0.04 ^{a*}
Day 7	28.78 \pm 7.41	21.56 \pm 8.76	24.78 \pm 28.78	0.661 ^b
Day 14	22.11 \pm 4.07	23.33 \pm 4.67	26.66 \pm 5.77	0.479 ^a
p-value	0.430 ^a	0.060 ^a	0.731 ^b	

SD: standard deviation

^aAnalyzed using Anova test

^bAnalyzed using Kruskal-Wallis test

*Statistically significant at $p < 0.05$

Histopathological analysis

Histopathological analysis on day 3 revealed that fibroblast infiltration was significantly lower in the parietal peritoneum group compared to the other groups. However, by day 14, fibroblast number and tissue organization had improved in all groups, with no significant intergroup

differences. The control group showed progressive fibroblast activity and neo-tissue formation. The parietal peritoneum group exhibited delayed fibroblast infiltration but gradual tissue remodeling. Gallbladder graft group had robust fibroblast activity and vascularization by day 7, with organized tissue by day 14 (**Figure 4**). In the parietal peritoneum group, histological changes are presented in **Figure 5**. On day 3, sparse fibroblasts were observed, suggesting early healing, and on day 7 fibroblast density was increased, reflecting active tissue remodeling. By day 14 (**Figure 5C**), fibroblast density was stabilized with organized tissue, indicating maturation.

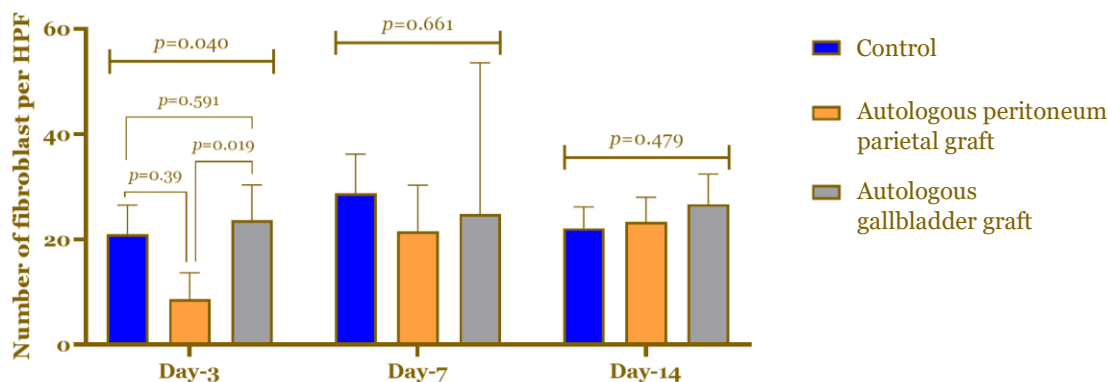


Figure 4. Mean number of fibroblasts per selected high-power fields (HPFs) between experimental groups across different time points.

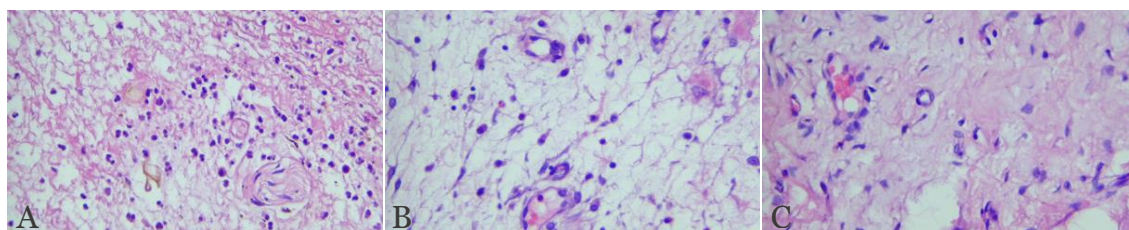


Figure 5. Representative qualitative histopathological analysis tissue from animal within parietal peritoneum graft group stained with hematoxylin and eosin (H&E) with 300 \times magnification on day 3 (A), day 7 (B) and day 14 postoperative (C).

Discussion

This study explored the effects of autologous parietal peritoneum grafts on BDI in animal models, focusing on the levels of CD68 and TGF- β as key markers of inflammation and fibrosis. The results demonstrated the graft's potential in bile duct repair by facilitating tissue remodeling, balancing inflammatory responses, regulating macrophage and fibroblast activity, and promoting early TGF- β elevation with normalization by day 14, indicative of successful integration. Histological analysis further supported its efficacy as a structural scaffold for effective healing and tissue restoration.

The incidence of BDI has increased with the increased use of laparoscopic cholecystectomy, currently observed in 0.3–0.7% of the approximately 750,000 procedures performed annually in the United States [16]. The management of BDI is stratified based on the type and severity of the injury [17]. Simple bile leaks, categorized as Strasberg type A, are effectively treated through minimally invasive techniques such as primary suturing and stent placement via endoscopic retrograde cholangiopancreatography [18]. However, complex injuries, particularly those classified as Strasberg types E1 to E3, necessitate advanced surgical interventions like Roux-en-Y hepaticojejunostomy [19]. While this approach achieves a high success rate, its complications, including intestinal reflux, hormonal dysregulation, and recurrent biliary infections, pose significant challenges to long-term patient outcomes [20].

This study evaluated the feasibility of autologous parietal peritoneum grafts for the repair of partial BDIs. The parietal peritoneum, characterized by its regenerative and anti-inflammatory properties, serves as a promising graft material. Its mesothelial layer, rich in stem cell-derived

components, actively secretes extracellular matrix proteins, cytokines, and growth factors critical for tissue repair [21]. Additionally, its partial embryological connection to the bile duct, through their shared mesodermal origin in supporting tissues, enhances its biocompatibility and integration, while its accessibility minimizes donor site morbidity [22,23]. Together, these attributes position the parietal peritoneum as an innovative and practical solution for bile duct reconstruction.

The biological process of wound healing is inherently dynamic, involving a coordinated sequence of inflammation, cellular recruitment, and tissue remodeling. Macrophages, identified through CD68 expression, are pivotal in mediating these phases. Their dual phenotype—pro-inflammatory (M1) and anti-inflammatory (M2)—ensures effective debris clearance, inflammation resolution, and promotion of tissue regeneration [24]. The inflammatory cytokines tumor necrosis factor-alpha (TNF- α) and interleukin-1 beta (IL-1 β) play a crucial role in recruiting immune cells to the injury site and initiating angiogenesis. This process is mediated by vascular endothelial growth factor (VEGF) signaling through its receptors VEGFR-1 and VEGFR-2 on endothelial cells, with VEGFR-2 activation driving critical downstream pathways such as Ras-Raf-MEK-ERK and PI3K-Akt. These pathways collectively enhance vascularization and support the structural and functional restoration of injured bile duct tissue [25].

This study demonstrated consistent CD68 expression across all experimental groups, indicating that autologous grafts effectively support macrophage recruitment without exacerbating inflammation. On day 3, macrophages played a pivotal role in clearing cellular debris and preventing infection, critical steps for initiating wound healing. By day 7, there was a notable shift from M1 to M2 macrophages, which aligned with the transition from the inflammatory phase to tissue proliferation. This shift is essential for promoting tissue regeneration while minimizing excessive inflammation. By day 14, macrophage activity reached a resolution phase, with CD68 levels stabilizing across all groups, underscoring the autologous graft's ability to mediate controlled immune responses. This highlights the grafts' potential to limit chronic inflammation and fibrosis while promoting effective tissue remodeling and regeneration.

TGF- β is a pivotal cytokine in wound healing, exerting a dual role in both initiating tissue repair and orchestrating extracellular matrix synthesis [26]. In the early stages of wound healing, TGF- β promotes the recruitment of fibroblasts to the site of injury, a process primarily facilitated through the fibronectin pathway [27]. This cytokine also plays a critical role in angiogenesis, balancing proangiogenic and antiangiogenic factors to promote blood vessel formation [28]. Moreover, TGF- β is integral to extracellular matrix synthesis formation, ensuring proper tissue regeneration and repair [29]. In the present study, TGF- β levels were notably elevated in the autologous peritoneum group on day 3, underscoring its role in facilitating fibroblast migration and tissue repair initiation. The temporal rise in TGF- β concentration highlights its involvement in the early stages of wound healing. By day 14, TGF- β levels had returned to baseline across all groups, marking the resolution of the proliferative phase and the commencement of tissue remodeling. This normalization of TGF- β levels suggests that autologous peritoneum grafts mimic the healing trajectory seen in conventional primary closure, while potentially accelerating early repair mechanisms. These findings emphasize the therapeutic potential of autologous peritoneum grafts in enhancing wound healing dynamics without compromising long-term repair outcomes.

Fibroblasts are essential in tissue repair, primarily through their role in extracellular matrix deposition and wound contraction [30]. Neutrophils, through the secretion of TNF- α and IL-1, facilitate the recruitment of epithelial cells and fibroblasts to the injury site. The proliferative response of fibroblasts is further stimulated by fibroblastic growth factors released during platelet degranulation [31]. In the present study, delayed fibroblast infiltration was observed in the autologous peritoneum group on day 3, suggesting an initial lag in cellular recruitment. However, by day 14, fibroblast density across all groups became comparable, indicating the graft's capacity to facilitate effective tissue remodeling. The delayed fibroblast response in the early phase can be attributed to the time required for graft integration and the modulation of inflammatory responses. Previous studies suggest that this delayed fibroblast activity may be related to the graft's early phase of integration, involving mechanisms such as immune modulation [32],

immune response [33], neovascularization [34], and fibroblast recruitment [35]. These factors contribute to a temporally regulated, orchestrated healing process, ensuring that fibroblast proliferation and tissue repair are not prematurely overstimulated.

The initial delay in fibroblast activity, followed by increased tissue organization by day 14, suggested that the autologous parietal peritoneum graft effectively supports bile duct repair. Histological analysis confirmed its role as a scaffold for fibroblast activity, promoting tissue regeneration. This underscores the graft's potential as an alternative to primary closure for partial BDIs. By maintaining balanced inflammation and fibroblast activity, alongside TGF- β regulation, the graft fosters effective tissue healing and remodeling. Its ability to avoid prolonged inflammation and immune reactions highlights its biocompatibility and safety, making it a promising solution in cases where primary closure is unfeasible. The autologous peritoneum graft offers a biologically compatible approach, potentially improving patient outcomes by reducing complications.

This study has some limitations that need to be discussed, including a short follow-up period that did not address long-term complications, such as graft durability. The small sample size and animal model further limit generalizability to human cases. Future research should focus on long-term evaluations, clinical trials, and further exploration of molecular pathways to optimize graft integration and healing.

Conclusion

This study highlights the promising potential of autologous parietal peritoneum grafts in the repair of partial BDIs. The graft facilitated effective tissue remodeling, supported by balanced inflammatory responses, controlled macrophage activity (CD68), and regulated fibroblast infiltration and activity. Elevated TGF- β levels in the early phase underscored the graft's ability to promote tissue repair, with normalization by day 14 indicating successful integration and remodeling akin to primary closure. Histological analysis further confirmed the graft's suitability as a structural scaffold for healing.

Ethics approval

This study was conducted in compliance with the ethical guidelines for animal research and was approved by the Institutional Review Board of the Ethics Committee of Dr. Moewardi General Hospital, Surakarta, Indonesia (approval number: 1.785/X/HREC/2023).

Acknowledgments

The authors would like to acknowledge Prof. Soeparwi Veterinary Hospital, Faculty of Veterinary Medicine, Universitas Gadjah Mada, for providing animal care facilities; the Biomedical Laboratory, Faculty of Medicine, Universitas Sebelas Maret, for technical support; and the Anatomical Pathology Laboratory, Faculty of Medicine, Universitas Gadjah Mada, for assistance with pathological analyses.

Competing interests

All the authors declare that there are no conflicts of interest.

Funding

This study received no external funding.

Underlying data

Derived data supporting the findings of this study are available from the corresponding author on request.

Declaration of artificial intelligence use

We hereby confirm that no artificial intelligence (AI) tools or methodologies were utilized at any stage of this study, including during data collection, analysis, visualization, or manuscript

preparation. All work presented in this study was conducted manually by the authors without the assistance of AI-based tools or systems.

How to cite

Nugroho AN, Mudigdo A, Soetrisno S, *et al.* Evaluating autologous peritoneum grafting for enhanced healing of bile duct injuries: A preliminary data from an animal study. *Narra J* 2025; 5 (1): e1873 - <http://doi.org/10.52225/narra.v5i1.1873>.

References

- Vincenzi P, Mocchegiani F, Nicolini D, *et al.* Bile duct injuries after cholecystectomy: An individual patient data systematic review. *J Clin Med* 2024;13(16):4837.
- Coletta D, Mascioli F, Balla A, *et al.* Minilaparoscopic cholecystectomy versus conventional laparoscopic cholecystectomy: An endless debate. *J Laparoendosc Adv Surg Tech* 2021;31(6):648-656.
- Schreuder AM, Busch OR, Besselink MG, *et al.* Long-term impact of iatrogenic bile duct injury. *Dig Surg* 2020;37(1):10-21.
- Keyur B, Pankaj D, Dhaval M, Daxa K. Bile duct injury: Surgical use of endobiliary stents for the management in emergency situations. *Indian J Surg* 2021;83(5):1146-1152.
- Marichez A, Adam JP, Laurent C, Chiche L. Hepaticojejunostomy for bile duct injury: State of the art. *Langenbeck's Arch Surg* 2023;408(1):107.
- Zheng F, Zhang Y, Ha L, *et al.* Biliary reconstruction with localized creation: One case report of repairing bile duct injury and defect with autografts. *Int J Surg Case Rep* 2024;118:109597.
- Asaoka T, Furukawa K, Mikamori M, *et al.* Portal vein wedge resection and patch venoplasty with autologous vein grafts for hepatobiliary-pancreatic cancer. *Surg Case Reports* 2024;10(1):27.
- Li J, Lü Y, Qu B, *et al.* Application of a new type of sutureless magnetic biliary-enteric anastomosis stent for one-stage reconstruction of the biliary-enteric continuity after acute bile duct injury: An experimental study. *J Surg Res* 2008;148(2):136-142.
- Cheng Y, Xiong XZ, Zhou RX, *et al.* Repair of a common bile duct defect with a decellularized ureteral graft. *World J Gastroenterol* 2016;22(48):10575.
- Han HJ, Kim KC, Yoon HY. Case report: Surgical correction of a cystic duct stump leakage following cholecystectomy using an autologous rectus sheath graft in a dog. *Front Vet Sci* 2021;8:584975.
- Bonvini S, Albiero M, Ferretto L, *et al.* The peritoneum as a natural scaffold for vascular regeneration. *PLoS One* 2012;7(3):e33557.
- Lapergola A, Felli E, Rebiere T, *et al.* Autologous peritoneal graft for venous vascular reconstruction after tumor resection in abdominal surgery: a systematic review. *Updates Surg* 2020;72(3):605-615.
- Chen B, Chen X, Wang W, *et al.* Tissue-engineered autologous peritoneal grafts for bladder reconstruction in a porcine model. *J Tissue Eng* 2021;12:2041731420986796.
- Raffea NM, Allawi AH. Effect of autologous peritoneum and platelet-rich fibrin graft on healing of intestinal anastomosis in dogs. *Iraqi J Vet Sci* 2022;36(2):459-470.
- Johns Hopkins University Animal Care and Use Committee. Guidelines. Available from: <https://animalcare.jhu.edu/guidelines/>. Accessed: 5 February 2024.
- Dhanasekara CS, Shrestha K, Grossman H, *et al.* A comparison of outcomes including bile duct injury of subtotal cholecystectomy versus open total cholecystectomy as bailout procedures for severe cholecystitis: A multicenter real-world study. *Surg* 2024;176(3):605-613.
- Chun K. Recent classifications of the common bile duct injury. *Korean J Hepatobiliary Pancreat Surg* 2014;18(3):69.
- Garcés-Albir M, Martí-Fernández R, Martínez-Fernández G, *et al.* The role of endoscopic retrograde cholangiopancreatography in the management of iatrogenic bile duct injury after cholecystectomy. *Rev Esp Enfermedades Dig* 2019;111(9):690-695.
- Lalisang TJM, Situmorang I, Ibrahim F, *et al.* Management of post-cholecystectomy bile duct injuries without operative mortality at Jakarta tertiary hospital in Indonesia – A cross-sectional study. *Ann Med Surg* 2021;62:211-215.
- Meadows V, Baiocchi L, Kundu D, *et al.* Biliary epithelial senescence in liver disease: There will be SASP. *Front Mol Biosci* 2021;8:803098.

21. Castillo JM, Flores-Plascencia A, Perez-Montiel MD, *et al.* Parietal peritoneum graft for duodenum injuries in an animal model. *Arq Bras Cir Dig* 2019;32(1):e1418.
22. Roskams T, Desmet V. Embryology of extra- and intrahepatic bile ducts, the ductal plate. *Anat Rec* 2008;291(6):628-635.
23. Mutsaers SE. Mesothelial cells: Their structure, function and role in serosal repair. *Respirology* 2002;7(3):171-191.
24. Kong C, Zhang C, Wu Y, *et al.* The expression and meaning of CD68, CD163, CD57, and IgG4 in granulomatous lobular mastitis. *Gland Surg* 2020;9(4):936-949.
25. Wang X, Labzin LI. Inflammatory cell death: How macrophages sense neighbouring cell infection and damage. *Biochem Soc Trans* 2023;51(1):303-313.
26. Budi EH, Schaub JR, Decaris M, *et al.* TGF- β as a driver of fibrosis: Physiological roles and therapeutic opportunities. *J Pathol* 2021;254(4):358-373.
27. Deng Z, Fan T, Xiao C, *et al.* TGF- β signaling in health, disease, and therapeutics. *Signal Transduct Target Ther* 2024;9(1):61.
28. Liu ZL, Chen HH, Zheng LL, *et al.* Angiogenic signaling pathways and anti-angiogenic therapy for cancer. *Signal Transduct Target Ther* 2023;8(1):198.
29. Massagué J, Sheppard D. TGF- β signaling in health and disease. *Cell* 2023;186(19):4007-4037.
30. Cialdai F, Risaliti C, Monici M. Role of fibroblasts in wound healing and tissue remodeling on Earth and in space. *Front Bioeng Biotechnol* 2022;10:958381.
31. Soliman AM, Barreda DR. Acute inflammation in tissue healing. *Int J Mol Sci* 2022;24(1):641.
32. Kupusovic J, Kessler L, Kazek S, *et al.* Delayed 68Ga-FAPI-46 PET/MR imaging confirms ongoing fibroblast activation in patients after acute myocardial infarction. *IJC Hear Vasc* 2024;50:101340.
33. Raziyeva K, Kim Y, Zharkinbekov Z, *et al.* Immunology of acute and chronic wound healing. *Biomolecules* 2021;11(5):700.
34. Stańczak M, Kacprzak B. Molecular biology of ACL graft healing: Early mechanical loading perspective. *Preprints* 2024:2024081117.
35. Yao S, Fu BSC, Yung PSH. Graft healing after anterior cruciate ligament reconstruction (ACLR). *Asia Pac J Sports Med Arthrosc Rehabil Technol* 2021;25:8-15.